Measurement of the Mean Inner Potentials of Anthracene and Naphthalene

Richard R. Lunt,[1,2] Stéphane Kéna-Cohen,[1,2] Jay B. Benziger,[1] and Stephen R. Forrest[2,*]

[1]*Department of Chemical Engineering, Princeton Institute for the Science and Technology of Materials (PRISM), Princeton University, Princeton, New Jersey 08544, USA*

[2]*Departments of Electrical Engineering & Computer Science, Physics, and Materials Science & Engineering, University of Michigan, Ann Arbor, Michigan 48109, USA*

(Received 8 September 2008; published 13 February 2009)

The mean inner potential in metals, insulators, and semiconductors provides fundamental information regarding the electronic structure of the material. Here, we measure the mean inner potentials of the two archetype linear polyacenes: anthracence and naphthalene. We determine the mean inner potentials of single crystalline anthracene of 5.9 V (±0.3 V), and naphthalene of 5.4 V (±0.3 V) based on analysis of Kikuchi patterns observed using high-pressure reflection high energy electron diffraction. We show that the inner potential of a range of organic molecular semiconductors can be estimated from their diamagnetic susceptibilities.

DOI: 10.1103/PhysRevLett.102.065504 PACS numbers: 61.05.jh, 61.66.Hq, 71.20.Rv

The refraction of electron beams by a medium provides insight into its electronic structure. Refraction originates from the interaction of the incident electron with the mean inner (or Coulombic) potential (MIP) within a material. The MIP has been widely investigated using low energy electron diffraction [1], electron holography [2], reflection high energy electron diffraction [3], and can be related to a variety of material dependant properties such as work function [4,5] and ionicity of the solid [6]. Precise measurements of the MIP can also be used to evaluate the validity of the local density approximation in band structure calculations, which is especially significant for van der Waals bonded crystals [7]. While considerable effort has been focused on determining the MIP for inorganic materials such as metals [8,9], semiconductors [10,11], and insulators (including polystyrene and diamondlike carbon) [12–14], to our knowledge there have been no reports of its measurement for organic molecular crystals (OMCs). In part, this is likely due to limitations of various methods for measurement. For example, to our knowledge, there have been no reports of Kikuchi patterns or electron diffraction patterns deviating from the Bragg condition, while electron holography requires accurate determination of crystal shape and thickness, which can be difficult to achieve for OMCs. Furthermore, organic semiconductors often have high vapor pressures, can be difficult to grow into a large-area single crystal, and are susceptible to charging and beam damage under high beam currents required in electron diffraction experiments [15].

Here, we observe Kikuchi patterns using low-current and high-pressure reflection high energy electron diffraction (HP-RHEED) [16] for two organic materials, anthracene and naphthalene, grown as single crystals from the liquid phase, and use these data to extract their mean inner potentials.

The mean inner potential [see Fig. 1(a)] can be expressed as

$$V_0 = \frac{1}{\Omega}\int_{\text{cell}} V(\mathbf{r})d^3\mathbf{r}, \tag{1}$$

where $V(\mathbf{r})$ is the electrostatic potential due to the electron charge density, $\mathbf{r}$ is the position, and Ω is the unit cell volume. $V(\mathbf{r})$ is simplified by neglecting charge redistribution (the neutral-atom approximation), and a rough estimate of the inner potential can be obtained assuming a superposition of spherical atoms as [17]:

$$V_0 = \frac{h^2}{2\pi m_e q \Omega}\sum_i n_i f_i^{\text{el}}(s=0), \tag{2}$$

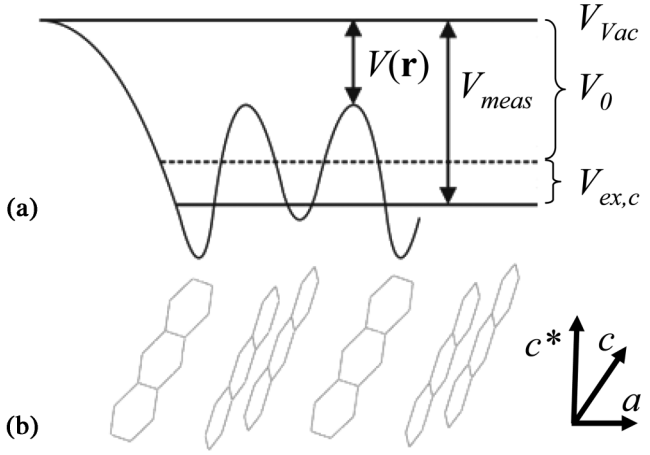

FIG. 1. Schematic representation of the position dependent electrostatic potential, $V(\mathbf{r})$, resulting from the charge density distribution along the a axis of an anthracene crystal. V_0, the mean inner potential, is a property of materials related to the surface dipole. The vacuum level, V_{vac}, and the measured potential, V_{meas}, are indicated, and the exchange-correlation potential, $V_{\text{ex},c}$, has been exaggerated for clarity. The measured potential has contributions from both the mean inner potential and exchange-correlation of the many-electron wave function in the material. This contribution is important with probing electron beams at low energy where $V_{\text{ex},c}$ is significant.

where f_i^{el} $(s = 0)$ is the electron scattering factor [18] at a scattering vector s for atom i, h is Planck's constant, m_e is the electron mass, q is the electronic charge, and n is the number of i atoms. Because of the sensitivity of Eq. (1) to charge redistribution, Eq. (2) often overestimates V_0 by 1 to 2 V. As will be shown below, this is indeed true for the acenes, and highlights the need for accurate measurements.

Rosenfeld has shown that the diamagnetic susceptibility can be related to the mean square radius for a gas atom [19], $\langle r_a^2 \rangle$. Again, assuming a superposition of spherical atoms, the volume susceptibility χ_V can then be related to the mean inner potential via

$$\chi_V = \chi_M \frac{\rho}{M} = -\frac{\mu_0 N q^2}{(4\pi)6m_e}\langle r_a^2 \rangle = \frac{q}{(4\pi)m_e c^2} V_0, \quad (3)$$

where c is the speed of light, N is Avagadro's number, μ_0 is the vacuum permeability, and the molar susceptibility χ_M is related to the volume susceptibility by the ratio of the density ρ to the molecular weight M. The diamagnetic susceptibility for a wide range of organic materials can be found in Ref. [20]. Although this equation was derived for gases, it has been shown that the molecular diamagnetic susceptibility of a material does not vary for differing thermodynamic states (i.e., solid, liquid, etc.) [21]. Moreover, the validity of this relationship for solid compounds was generally confirmed by Miyake [22] for a range of ionic materials.

Referring to Fig. 1, the measured MIP, V_{meas}, can be related to V_0 using [5]:

$$V_{\mathrm{meas}} = V_0 + V_{\mathrm{ex},c} = \Phi + \varepsilon_f. \quad (4)$$

Here, $V_{\mathrm{ex},c}$ is the exchange-correlation contribution, and for metals, it has been shown that the MIP can also be related to the work function Φ and the Fermi energy ε_f. At high incident electron energies (10–100 keV), Coulombic interactions dominate, and the exchange potential is small [5], leading to $V_{\mathrm{meas}} = V_0$ regardless of the material. Particularly, the exchange and correlation potentials for molecular semiconductors are likely to be negligible, as indicated by narrow bandwidths <100 meV [23].

Single crystalline anthracene and naphthalene films $(20 \times 20\ \mathrm{mm}^2)$ were prepared by heating two glass slides with a natural air gap of several microns in a boat of organic powder (>99.95% purity measured by mass spectrometry) above the melting points of 508 and 361 K. These structures were then cooled at 0.5 K/min and 0.1 K/min, respectively. After growth, the slides were separated to maintain a flat surface over most of the crystal area. Given that anthracene and naphthalene have room-temperature vapor pressures of approximately 0.1 and 80 m Torr, respectively, HP-RHEED was preformed at a nitrogen pressure of 10–30 m Torr, and at a temperature from 225 to 273 K to prevent film vaporization. Film damage was avoided by using low beam currents of 50 to 90 nA, at a beam energy and exposure time of 20.0 keV and 5–300 s, respectively. This corresponds to an electron dose range of 0.5 to 50 $\mathrm{C/m}^2$.

Since Kikuchi electrons appear to originate from the bulk, they undergo refraction when exiting the crystal that bends the pattern towards the shadow edge. If the crystal structure is known, these patterns can be fit to extract the mean inner potential and the shadow edge position. The diffraction condition is given by [24]:

$$\mathbf{k}_{||} \cdot \mathbf{G}_{||} + |\mathbf{k}_\perp||\mathbf{G}_\perp| = |\mathbf{G}(h, k, l)|^2/2, \quad (5)$$

where $\mathbf{k}_{||}$ and $\mathbf{k}_\perp$ are the electron wave vectors in the crystal parallel $(||)$ and perpendicular $(\perp)$ to the surface plane, respectively, and $\mathbf{G}(h, k, l) = \mathbf{G}_{||} + \mathbf{G}_\perp$ is the reciprocal lattice vector for lattice coordinates, (h, k, l). Accounting for the change in electron wave vector in the normal direction due to the inner potential, and including relativistic effects for the vacuum electron wave vector, $\mathbf{K}$, this expression can be written as [25]:

$$\theta_{||}(\mathbf{n}_{||} \cdot \mathbf{G}_{||}) + \left(\theta_\perp^2 + \frac{2V_0 m_e q c^2}{2E m_e c^2 + E^2}\right)|\mathbf{G}_\perp| = \frac{|\mathbf{G}(h, k, l)|^2}{2|\mathbf{K}|}, \quad (6)$$

where E is the incident electron energy and $\mathbf{n}_{||}$ is the reciprocal unit vector parallel to the plane of observation. The diffraction angles in the perpendicular and parallel directions, $\theta_\perp$ and $\theta_{||}$, are then referenced to those from a KBr single crystal.

From Eq. (6), the crystal structure must be measured to determine $\mathbf{G}$, since it is possible that strained growth may lead to deviations from the bulk structure. Also, the concurrent measurement of the unit cell volume (or density) along with the MIP can help to reduce the impact of sample preparation variability [14] and allow for accurate comparison of the MIP to other values. For anthracene, the in-plane lattice constants determined directly from the HP-RHEED patterns at various rotations (i.e., Fig. 2) were found to be 8.68×6.05 Å^2 $(\pm 0.06 \times 0.05$ Å$^2)$ at room temperature, which is slightly expanded compared to that of the bulk monoclinic structure [26] stacking with

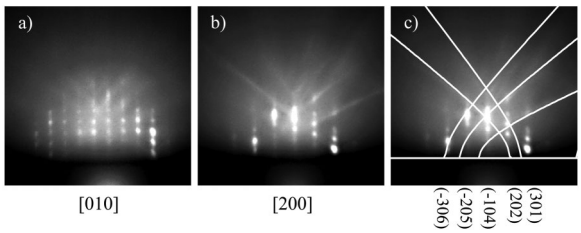

FIG. 2. HP-RHEED diffraction patterns of a single crystal anthracene film in the (a) [010] and (b) [200] directions. (c) The same pattern as (b) with the fitted Kikuchi pattern where the mean inner potential is $V_0 = (5.9 \pm 0.3)$ V. All patterns were obtained at 20.0 keV, <100 nA, and 10–30 m Torr background pressure and have been contrast-enhanced for clarity. Both Kikuchi lines and envelopes are clearly visible in (b).

the c^* axis normal to the substrate. This stacking was confirmed by both x-ray diffraction, where $c^* = 9.16$ Å, and from RHEED beam positions where the sample roughness yielded intensity variations along the diffraction streaks [i.e., Fig. 2(a)], yielding $c^* = 9.18$ Å(± 0.10 Å). The measured d spacings (from fitting RHEED patterns in several directions) were $d(100) = 7.13$ Å, $d(010) = 6.05$ Å, and $d(001) = 9.18$ Å. The measured unit cell volume and density were 475 Å^3 (± 5 Å^3) and 1.25 g/cm^3 (± 0.01 g/cm^3).

Naphthalene (Fig. 3) was found to stack similarly to anthracene with the c^* normal to the substrate. The measured d spacings at 225 K were found to be $d(100) = 7.14$ Å(± 0.05 Å), $d(010) = 6.10$ Å(± 0.07 Å), and $d(001) = 6.76$ Å(± 0.09 Å); the c parameter is shorter than in the bulk, while a and b are slightly larger. The thermal expansion coefficient [27] for naphthalene is approximately 1.5×10^{-4} K^{-1}, indicating the expected volume reduction of the crystal structure is approximately 12 Å^3, consistent with the observed reduction of 11 Å^3 from the room-temperature bulk unit cell volume of 361 Å^3. The measured unit cell volume and density are 350 Å^3 (± 6 Å^3) and 1.21 g/cm^3 (± 0.02 g/cm^3).

The Kikuchi patterns were fit to Eq. (6) using a nonlinear least squares algorithm after indexing each line. The resulting fits are shown in Figs. 2(c) and 3(c). An average value of the mean inner potential of $V_0 = 5.9$ V (± 0.3 V) was extracted for anthracene from fitting patterns from different samples. Within the uncertainty of the fitting procedure, this value was found to be independent of beam dose (up to at least 50 C/m^2), indicating that any charging effects on the measurement were negligible. The same procedure was used for fitting naphthalene patterns in the [100] direction, where the line indexing is nearly identical to that of anthracene. The extracted potential for naphthalene yielded $V_0 = 5.4$ V (± 0.3 V). The error for each MIP stems from the fitting uncertainty and variations from sample to sample.

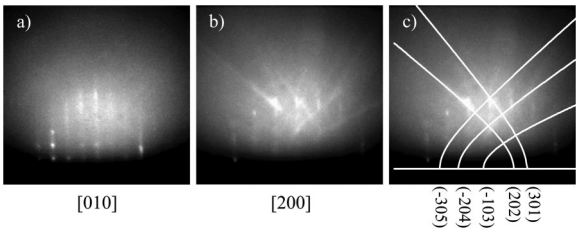

FIG. 3. HP-RHEED diffraction patterns of a single crystal naphthalene film at 225 K in the (a) [010] and (b) [200] directions. (c) The same pattern as (b) with the fitted Kikuchi pattern where the mean inner potential is $V_0 = (5.4 \pm 0.3)$ V. All patterns were obtained at 20.0 keV, <100 nA, and 10–30 m Torr background pressure, and have been contrast enhanced for clarity. Both Kikuchi lines and envelopes are clearly visible in (b).

Equations (2) and (3) suggest a linear relationship between V_0 and density, as is the case with most inorganic compounds. The predicted trends for molecular systems are shown in Fig. 4 including pyrene, perylene, coronene, and the linear acenes of benzene through pentacene. These values are also included in Table I. Equation (2) suggests that, similar to inorganic compounds, the valence shell contracts when carbon atoms are combined to form molecules; thus the neutral-atom approximation overestimates the electron density, and consequently the inner potential by approximately 1 V for both OMCs studied. Alternatively, the use of diamagnetic susceptibility data in combination with Eq. (3), provides a reasonably accurate estimate of the MIP and, therefore, could be used as an initial estimate when MIP measurements are not available. Moreover, since Eq. (3) suggests that the MIP should vary linearly with molecular density, or nearly equivalently valence electron density, then V_0 can be inferred in cases where neither diamagnetic susceptibility nor direct measurements are readily available. This situation obtains, for example, when diamagnetic and paramagnetic contributions to the magnetic susceptibility cannot be distinguished. Ultimately, the MIP can be used to estimate the work function, or exchange-correlation potentials provided that these parameters can be related to V_0 in a similar manner to metals.

In conclusion, we have demonstrated that Kikuchi diffraction patterns can be observed for single crystalline organic molecular films at or near room temperature via HP-RHEED. From these patterns, we have extracted the mean inner potentials for anthracene, 5.9 V (± 0.3) V, and

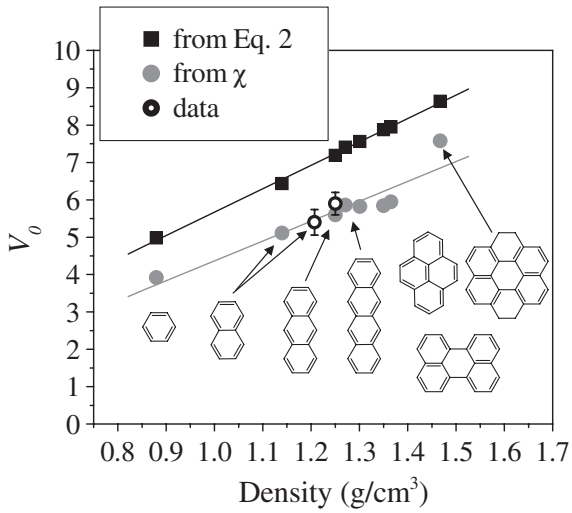

FIG. 4. The mean inner potential V_0 as a function of molecular density for a range of molecular semiconductors calculated from Eq. (2) (black squares), and from the diamagnetic susceptibility with Eq. (3) (gray circles). Experimental values are shown using open circles and are plotted against the measured densities from the HP-RHEED patterns. Diamagnetic susceptibility data and corresponding densities were obtained from Ref. [20].

TABLE I. Unit cell volumes (Ω), molar diamagnetic susceptibilities[a] (χ_M), and mean inner potentials (V_0) for common molecular organic semiconductors.

Molecule	Ω (Å^3)	χ_M (-1×10^6)	V_0 [Eq. (2)]	V_0 [Eq. (3)]	V_0 (Exp)
Benzene	294.8	54.5	4.98	3.92	...
Naphthalene	360.8[b]	90	6.55	5.11	5.4 ($\pm$0.3)[b]
Anthracene	476.2[b]	130	7.19	5.60	5.9 ($\pm$0.3)[b]
Pyrene	528.5	146	7.41	5.86	...
Tetracene	582.9	160	7.56	5.82	...
Perylene	620.8	171	7.88	5.85	...
Pentacene	677.3	190	7.95	5.95	...
Coronene	680.0	243	8.64	7.58	...

[a] χ_M obtained from Ref. [20].
[b] The measured cell volumes are 350 ($\pm$5) Å^3 and 475 ($\pm$5) Å^3 for naphthalene and anthracene, respectively.

naphthalene, 5.4 V ($\pm$0.3 V). These values are consistent with the values derived from diamagnetic susceptibilities for a range of polyacenes. While no clear connection exists between the mean inner potential and work function for semiconductors, as there is for metals, further theoretical treatment could lead to the useful extraction of the work function from diamagnetic susceptibility data.

The authors thank N. C. Giebink and Dr. M. S. Arnold for many helpful discussions, and the Air Force Office of Scientific Research for partial financial support of this work.

*stevefor@umich.edu

[1] W. Qian, J. C. H. Spence, and J. M. Zuo, Acta Crystallogr. Sect. A **49**, 436 (1993).
[2] J. Cai, F. A. Ponce, S. Tanaka, H. Omiya, and Y. Nakagawa, Phys. Status Solidi A **188**, 833 (2001).
[3] W. Braun, L. Daweritz, and K. H. Ploog, Phys. Rev. Lett. **80**, 4935 (1998).
[4] J. B. Pendry, J. Phys. C **2**, 1215 (1969).
[5] D. K. Saldin and J. C. H. Spence, Ultramicroscopy **55**, 397 (1994).
[6] L. M. Peng, S. L. Dudarev, and M. J. Whelan, Phys. Rev. B **56**, 15314 (1997).
[7] W. F. Perger, Chem. Phys. Lett. **368**, 319 (2003).
[8] A. Goswami and N. D. Lisgarten, J. Phys. C **15**, 4217 (1982).
[9] M. A. Ochando, A. Sanchez, and C. R. Serna, J. Phys. C **16**, L401 (1983).
[10] P. Kruse, M. Schowalter, D. Lamoen, A. Rosenauer, and D. Gerthsen, Ultramicroscopy **106**, 105 (2006).
[11] J. Li, M. R. McCartney, R. E. Dunin-Borkowski, and D. J. Smith, Acta Crystallogr. Sect. A **55**, 652 (1999).
[12] Y. C. Wang, T. M. Chou, M. Libera, E. Voelkl, and B. G. Frost, Microsc. Microanal. **4**, 146 (1998).
[13] C. A. Murison, Philos. Mag. **17**, 201 (1934).
[14] D. Shindo, T. Musashi, Y. Ikematsu, Y. Murakami, N. Nakamura, and H. Chiba, J. Electron Microsc. **54**, 11 (2005).
[15] S. R. Forrest, Chem. Rev. **97**, 1793 (1997).
[16] R. R. Lunt, J. B. Benziger, and S. R. Forrest, Appl. Phys. Lett. **90**, 181932 (2007).
[17] M. Y. Kim, J. M. Zuo, and J. C. H. Spence, Phys. Status Solidi A **166**, 445 (1998).
[18] J. A. Ibers, Acta Crystallogr. **11**, 178 (1958).
[19] L. Rosenfeld, Naturwissenschaften **17**, 49 (1929).
[20] *CRC Handbook of Chemistry and Physics*, edited by David R. Lide (CRC Press, Ann Arbor, MI, 1992), 73rd ed.
[21] A. Bose, Philos. Mag. **21**, 1119 (1936).
[22] S. Miyake, Proc. Phys. Math. Soc. Jpn. **22**, 666 (1940).
[23] K. Hannewald, V. M. Stojanovic, J. M. T. Schellekens, P. A. Bobbert, G. Kresse, and J. Hafner, Phys. Rev. B **69**, 075211 (2004).
[24] M. Gajdardziskajosifovska and J. M. Cowley, Acta Crystallogr. Sect. A **47**, 74 (1991).
[25] And approximating $\sin(\theta)$ as θ for the small range of diffraction angles.
[26] R. B. Campbell, J. Trotter, and J. M. Robertson, Acta Crystallogr. **14**, 705 (1961).
[27] S. Haas, B. Batlogg, C. Besnard, M. Schiltz, C. Kloc, and T. Siegrist, Phys. Rev. B **76**, 205203 (2007).